Astron. Astrophys. 361, 952–958 (2000)

ASTRONOMY AND ASTROPHYSICS

The history and source of mass-transfer variations in AM Herculis

F.V. Hessman[1], **B.T. Gänsicke**[1], **and J.A. Mattei**[2]

[1] Universitäts-Sternwarte, Geismarlandstrasse 11, 37083 Göttingen, Germany
[2] American Association Variable Star Observers, 25 Birch St., Cambridge, MA, USA

Received 14 March 2000 / Accepted 14 August 2000

Abstract. The optical brightness of magnetic cataclysmic variables without accretion discs is a direct measure of the near-instantaneous mass-transfer rates from the late-type secondary stars to the magnetic white dwarfs in these semi-detached binary systems. We derive the mass-transfer history of the magnetic cataclysmic variable AM Herculis from its long-term visual light curve and from bolometric corrections obtained from a number of X-ray observations covering various accretion states. On average, less than 25% of the maximum observed mass-transfer rate occurs. Assuming that the mass-transfer rate is modulated by stellar starspots on the secondary stars, we convert the derived mass-transfer rates into spot filling factors at the L_1-point. A statistical model for the coverage fraction and size distribution of random spots near the L_1-point in AM Her suggests that the spot filling factor is roughly 0.5 for a fitted power-law distribution of starspot radii, i.e. about half the surface of the star near the L_1-point is covered with spots. This density can only be explained if the spottedness of the L_1-point is unusual – for instance if spot groups are forced to wander towards the L_1-point – or if a large-scale magnetic spot group produced by an α^2-dynamo slowly drifts in and out of the L_1-region. The former solution predicts that the occurrence of long-term high- and low-states is random and the latter that the long-term light curves of polars are quasi-periodic; the light curve of AM Her may suggest periods of order a decade. Finally, we discuss the relevance of this result to the mass-transfer variations of other cataclysmic variables.

Key words: accretion, accretion disks – stars: binaries: general – stars: individual: AM Her – stars: magnetic fields – stars: novae, cataclysmic variables

1. Introduction

Cataclysmic variables (CV) of the AM Her or "polar" subclass consist of late-type secondary stars in semi-detached orbits around highly magnetic white dwarfs. The secondary loses mass via the L_1-point at a rate which is set by the scale height and density of the secondary's atmosphere within the L_1-region. The lost matter falls in the potential well of the primary until it is captured by and accreted along the white dwarf's magnetic field. Strong fields can prevent the formation of an accretion disc, so – without a disc acting as a buffer for the transferred mass – the mass-transfer rate from the secondary nearly equals the instantaneous mass-accretion rate onto the white dwarf, i.e. $\dot{M}_{\rm acc}^{\rm wd} \approx \dot{M}_{\rm loss}^{\rm sec}$ (the free-fall time is $\ll$ a day).

None of the known polars show signs of nearly constant mass-transfer rates. The optical long-term light curve of the best-observed polar, AM Herculis itself, is shown in Fig. 1. Typical of many polars, there are long periods of up to hundreds of days during which the mass-accretion (and hence mass-transfer) rates are stably either very high or very low, and other times during which the system varies erratically on timescales down to a day. There are no obvious correlations between the appearance or properties of the extreme states and the orbital or magnetic properties of the system (e.g. masses, mass-ratios, orbital periods, magnetic moments).

Extended "low-states" are seen in a large fraction of all CV's: they occur in *all* well-observed polars, a sizeable fraction of novalike variables, and in some SU UMa subtype dwarf novae and intermediate polars. The durations of such states range from days to years and occur at irregular intervals. AM Her occasionally drops into low-states within a few days, so that the transition from a higher state to a low-state marks a significant and dramatic change in the accretion behaviour (see Warner 1999 and Hessman 2000 for recent reviews of the phenomenology of low-states). In novalikes, it appears that the extended low-states are created by the combination of very low mass-transfer rates and the heating of the inner discs in systems with hot white dwarfs (Leach et al. 1999).

Livio & Pringle (1994) discuss several models for the origin of mass-transfer (as opposed to mass-accretion) variations and conclude that starspots at the L_1-point are the most likely explanation. Given that CV secondaries are rapidly rotating late-type stars with a partially or fully convective inner structure, $\alpha-\omega$ or α^2 dynamos should result in intensive spottedness. In order to maintain pressure equilibrium with the surrounding photosphere, the spots have to have a lower thermal pressure, i.e. a lower temperature and/or density. The density in the spot at the level of the surrounding photosphere and, hence, the mass-

Send offprint requests to: hessman@uni-sw.gwdg.de

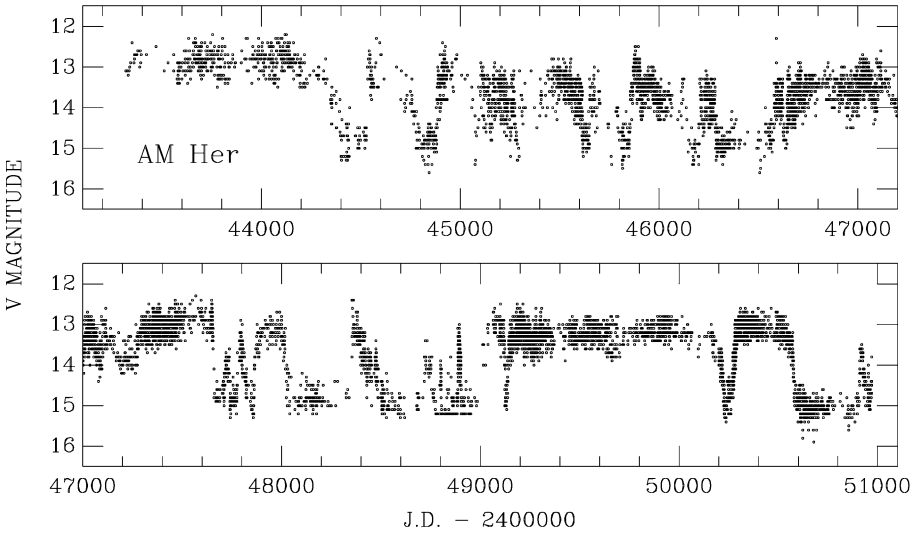

Fig. 1. Visual light curve of AM Her from June 1977 to May 1998, obtained from the archives of the AAVSO.

transfer rate through such a spot may be lower by several orders of magnitude.

In the next section, we take archival X-ray data and the visual observations of many dedicated amateur astronomers and construct the recent mass-transfer history of AM Her. In the following section, the statistical properties of this history are derived, permitting us to construct a statistical model of the spottedness. Finally, we discuss what physical consequences the simulated spot distribution has for the observed properties of AM Her and other cataclysmic variables.

2. Deriving the mass-transfer history

In order to derive the *mass-transfer* history of the secondary star in AM Her, we must first derive the *mass-accretion* history from the available observations at many times and wavelengths. The bulk of the gravitational energy released in an accreting polar is emitted in the X-ray regime, partly as optically thick quasi-blackbody radiation from the heated white dwarf atmosphere in regions of high local mass-flow densities, partly as optically thin bremsstrahlung from the stand-off shock in regions of relatively low accretion densities. In addition to the bremsstrahlung, the hot post-shock plasma emits cyclotron radiation in the visual/IR. Only about half of the bremsstrahlung/cyclotron emission is radiated away directly, the other half is intercepted by the white dwarf surface and either reflected or reprocessed into the UV range, as evidenced by a large heated spot around the main accretion region (Gänsicke et al. 1995,1998). At low accretion rates, one sees the photospheric flux of the (heated) white dwarf. Finally, the accretion stream can be a source of largely optically thin emission in the visual/UV wavelength range.

It is clear that a dense sampling of multi-wavelength observations of AM Her would be desirable to determine the temporal variation of all individual accretion flux components. However, the prime observational parameter which is available is the brightness at optical wavelengths. The intense visual monitoring of AM Her by the observers of the AAVSO resulted in more than 10 000 individual brightness estimates for the last 20 years. Fig. 1 shows the AAVSO data binned in 10 day intervals. $\dot{\mathrm{M}}_{\mathrm{loss}}^{\mathrm{sec}}$ can – in principle – be derived from Fig. 1 if the time-dependent accretion flux $F_{\mathrm{acc}}(t)$ can be expressed as a function of V. In a first approximation, we neglect the emission from the accretion stream and write

$$F_{\mathrm{acc}} = F_{\mathrm{SX}} + F_{\mathrm{HX}} + F_{\mathrm{cyc}} + F_{\mathrm{UV}} \quad (1)$$

where F_{SX}, F_{HX}, and F_{cyc} are the observed soft X-ray, thermal bremsstrahlung, and cyclotron fluxes, respectively. F_{UV} is the flux of the reprocessed emission from the heated pole cap. Gänsicke et al. (1995) have shown that in AM Her F_{HX}, F_{cyc}, and F_{UV} are of the same order of magnitude both during the high state and during the low state. Thus, it is possible to estimate

$$F_{\mathrm{acc}} \approx F_{\mathrm{SX}} + 3 \times F_{\mathrm{HX}} \quad (2)$$

from X-ray observations alone. The main uncertainty in our estimates of F_{acc} is not the approximation involved in the second term but the systematic uncertainties in the parameters of the dominant first term in Eq. 2, the bolometric value of the soft X-ray flux.

We have compiled values for F_{acc} from the literature based on observations with ROSAT (Gänsicke et al. 1995), BeppoSAX (de Martino et al. 1998), and EXOSAT (Paerels et al. 1994). Fig. 2 shows F_{acc} as function of the visual magnitude V, where the values of V for the individual X-ray observations were obtained from the AAVSO data. F_{acc} varies smoothly over a wide range in $V \approx 12.5$–15. For $V \lesssim 15$, F_{acc} drops steeply as the emission of AM Her approaches that of the underlying stellar components, indicating that accretion nearly ceases. We approximated the $F_{\mathrm{acc}}(V)$ distribution with two separate linear fits to the ranges $V > 15$ and $V \leq 15$.

With $F_{\mathrm{acc}}(V)$ known, we compute the accretion luminosity

$$L_{\mathrm{acc}}(V) = 4\pi d^2 F_{\mathrm{acc}}(V) \quad (3)$$

with $d = 90$ pc the distance of AM Her (Gänsicke et al. 1995). The assumption of isotropic emission may overestimate the accretion luminosity somewhat. As all values of F_{acc} are orbital

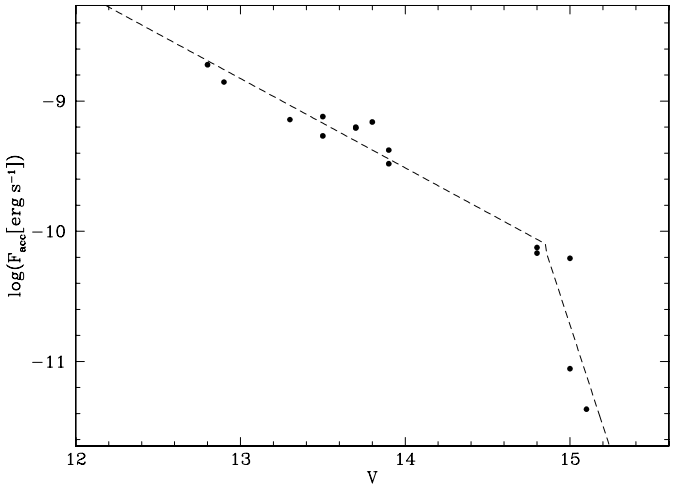

Fig. 2. Correlation between the visual magnitude and the accretion flux in AM Her. Plotted as dashed lines are two linear fits for $V < 15$ and $V \geq 15$.

mean values, this uncertainty does, however, not exceed a factor of 2, and is probably less as we neglected the emission of the accretion stream.

From $L_{\rm acc}$, we finally compute

$$\dot{\rm M}^{\rm sec}_{\rm loss}(V) = \frac{L_{\rm acc}(V) R_{\rm wd}}{G M_{\rm wd}} \tag{4}$$

with $R_{\rm wd} = 8.4 \times 10^8$ cm the adopted white dwarf radius, $M_{\rm wd} = 0.6\,{\rm M}_\odot$ the adopted white dwarf mass, and G the gravitational constant. $\dot{\rm M}^{\rm sec}_{\rm loss}(V)$ is shown in Fig. 3 (contiguous 10 day bins are connected by lines). The average value of $\dot{\rm M}^{\rm sec}_{\rm loss}$ is $7.9 \times 10^{15}{\rm g\,s^{-1}}$, or $1.2 \times 10^{-10}\,{\rm M_\odot yr^{-1}}$.

Hereafter, we will use $\dot{\rm M}$ to denote either the instantaneous mass-transfer or mass-accretion rate, on the assumption that they are effectively the same for our purposes.

3. Statistical properties

The simplest description of the statistical properties of the mass-transfer history is the differential probability $Prob(\dot{\rm M})$ of having a particular mass-transfer rate $\dot{\rm M}$. For convenience, we will use the relative mass-transfer rate $1 - \eta \equiv \dot{\rm M}/\dot{\rm M}_{\rm max}$, where $\dot{\rm M}_{\rm max} \approx (2.4 \pm 0.5) \cdot 10^{16}$ g s^{-1} (Fig. 3) and η is the relative "spottedness" (i.e. 0 if no spots are present and 1 if spots block the mass-transfer completely). $Prob(\eta)$ is derivable from the cumulative probability distribution function $C(\eta)$, defined as

$$C(\eta) \equiv \int_o^\eta Prob(\eta')d\eta',\ C(0) \equiv 0,\ C(1) \equiv 1. \tag{5}$$

$C(\eta)$ can be trivially derived from the observed values of η by noting that it is simply one minus the rank of the sorted η values divided by the number of measurements minus one.

The observed $C(\eta)$ and $Prob(\eta)$ curves for AM Her are shown in Fig. 4. Note that the median value of η ($C(\eta) = 0.5$) is 0.75, *i.e. on average, the L_1-point in AM Her yields no more than 25% of the observed mean maximum mass-transfer rate* and even less of the maximum ever observed rate. Local peaks in $Prob(\eta)$ – produced by smoothing and then differentiating $C(\eta)$ – are present at $\eta \approx 0.96{-}1.0$, $0.4{-}0.65$, and $0.77{-}0.88$, indicating that there are some propensities (of unknown origin) for certain mass-transfer rates.

4. Starspot-induced mass-transfer variations

The mass-transfer rate from the secondary through the L_1-point, $\dot{\rm M} = A_{L_1} \overline{\rho}_{L_1} c_{\rm s,2}$, depends upon the geometric radius, R_{L_1}, or cross-sectional area $A_{L_1} \equiv \pi R^2_{L_1}$ of the "nozzle" at the L_1-point

$$A_{L_1} = \frac{2\pi c_{\rm s,2} a^3}{G M_{\rm wd}(1+q)k(q)} \tag{6}$$

where a is the binary separation, q is the mass-ratio $M_2/M_{\rm wd}$, and $k(q) \approx 7$ (Meyer & Meyer-Hofmeister 1983), the mean mass-density $\overline{\rho}_{L_1}$ at the sonic point of the flow, and $c_{\rm s,2}$, the sound speed of the gas, approximately given by the isothermal sound speed at the effective temperature of the secondary. Following the discussion in Lubow & Shu (1975), the size of the nozzle can be fairly accurately expressed in terms of the characteristic dimensionless size of the flow

$$\epsilon \equiv \frac{c_{\rm s,2}}{\Omega_{\rm orb} a} \approx 0.003 \left(\frac{T_2}{4000{\rm K}}\right)^{1/2} \left(\frac{P_{\rm orb}}{1\,{\rm hr}}\right) \left(\frac{a}{10^{11}\,{\rm cm}}\right)^{-1} \tag{7}$$

where $\Omega_{\rm orb}$ is the orbital frequency. Since $A_{L_1} \approx \pi(\epsilon a/2)^2$, a typical value of R_{L_1} is about 2000 km.

The mean mass-density $\overline{\rho}_{L_1}$ is roughly given by the exponential fall-off of an isothermal atmosphere, $\overline{\rho}_{L_1} \approx \rho_o \exp(-\Delta R/H_2)$, where $\Delta R \equiv R_2 - R_{L_1}$ is the radial amount that the secondary overflows its Roche volume, and H_2 is the isothermal density scale height given by $H_2 \equiv \mathcal{R} T_2/g_{\rm eff}$, where $g_{\rm eff}$ is the effective gravity at the secondary's surface. The typical densities ρ_o can be derived in systems with known orbital parameters and accretion rates. For example, AM Her has $P_{\rm orb} = 3.09$ hr, $M_1 \approx 0.6\,{\rm M}_\odot$, $q \approx 0.45$, $T_2 \approx 3200$K, and $\dot{\rm M} < 4 \cdot 10^{-10}\,{\rm M_\odot yr^{-1}}$, resulting in $a \approx 7.1 \cdot 10^{10}$ cm, $\epsilon \approx 9.1 \cdot 10^{-3}$, $R_{L_1} \approx 3200$ km, and $\rho_o < 2 \cdot 10^{-7}\,{\rm g\,cm^{-3}}$.

We can simulate the spotted surface of AM Her's secondary star in an attempt to reproduce the statistical properties of the observed form of $C(\eta)$ by assuming that the L_1-point randomly samples the surface of a spotted region with uniform spot properties (i.e. spot depths and size distribution). The time-dependent mass-transfer curve can then be crudely thought of as the L_1-point's random-walk through the simulated spotted landscape. Lacking a detailed model for the spatial and density structure of spots in late-type dwarfs, we will assume that all spots have circular cross-sections with different radii $r = R_{\rm spot}$, that the radial increase in photospheric density away from the center of the spot is simply a Gauss function in r, and that no matter is lost from the very centers of the spots. In order to avoid a complex packing problem, we will also assume that individual spots can be arbitrarily superimposed spatially to produce spot groups whose depths are products of the individual spots. An example of such a spot simulation is shown in Fig. 6.

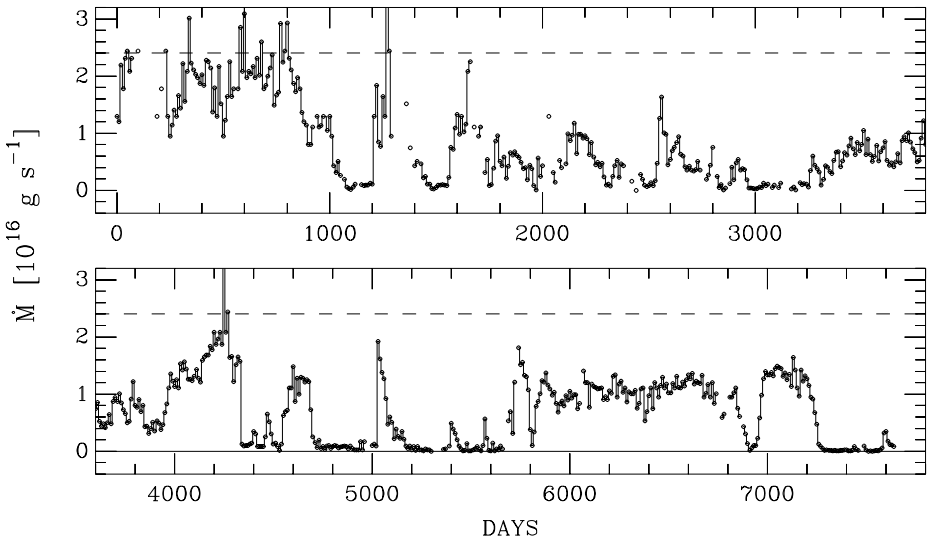

Fig. 3. The mass transfer rate in AM Her as a function of time (see Fig. 1). The dashed line indicates a reasonable value for the maximum quasi-stationary mass-transfer rate: $(2.4 \pm 0.5) \cdot 10^{16}$ g s^{-1} (i.e. $3.8 \cdot 10^{-10}$ M$_\odot$yr^{-1}).

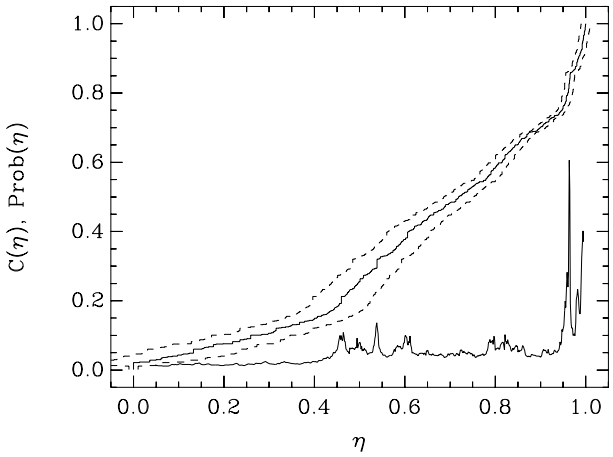

Fig. 4. The cumulative and differential probability distribution functions $C(\eta)$ and $Prob(\eta)$ for the relative spottedness $\eta \equiv 1-\dot{M}/\dot{M}_{\max}$ (Fig. 3). The dashed curves indicate the changes in $C(\eta)$ due to uncertainties in η.

We further assume that the distribution of spot sizes is a power-law in spot radius. The properties of the spotted area are then solely determined by: (1) the spot filling factor

$$f \;=\; 1 - \iint_{\rm Surface} \dot{\rm M}(x,y)dxdy \;/\; \iint_{\rm Surface} \dot{\rm M}_0\, dxdy \qquad (8)$$

where $\dot{\rm M}_0$ is the mass-transfer rate in the absence of starspots and f goes from 0 (no spots whatsoever) to 1 (star totally covered with "dark" spots and no matter transferred); (2) the power-law index γ of the spot size distribution function; and (3,4) the extreme spot radii $R_{\rm min}$ and $R_{\rm max}$.

The optimal parameter set was obtained by simulating many such spotted surfaces and then optimising the fit between the simulated and observed $C(\eta)$ using a modified version of the Press et al. (1992) simplex algorithm. The nominal errors were computed using the procedure outlined in Zhang et al. (1987), in which the error is derived by holding each parameter constant at a slightly different value and optimising the other parameters: $f = 0.53 \pm 0.04$, $\gamma = 1.98 \pm 0.08$, $R_{\rm min}/R_{L_1} = 0.12 \pm 0.40$, $R_{\rm max}/R_{L_1} = 2.91 \pm 0.04$. The resulting fit to the observed $C(\eta)$ data is shown in Fig. 5 along with other simulations with 5-σ changes in the parameters (for which the other parameters were not optimised). Not unexpectedly, the fitted geometry parameters – especially f, γ and $R_{\rm max}$ – are highly correlated: steeper spot size distributions (larger values of γ) require slightly higher values of f and/or larger maximum radii $R_{\rm max}$.

The fitted power-law solution does a fairly good job of reproducing the overall shape of the observed $C(\eta)$ (or rather $\eta(C)$) curve: the reduced χ^2-value of the fit is 0.45. However, the simple model is not able to reproduce the small-scale structure responsible for the local peaks in $Prob(\eta)$ (kinks in $C(\eta)$), particularly those around $\eta = 0.4-0.6$ caused by the middle-state "stand-still" phases (around 6000–7000 days in Fig. 3).

Fortunately, the filling factor – undoubtably the most important parameter describing the spottedness – is very well constrained: even totally random or fractal "spots" must have a filling factor not too far away from the observed value of η(C=0.5)=0.75 and our assumption of very dark (i.e. deep) spots minimises the spot filling factor needed to explain the mass-transfer history. We are unlikely to have *over-estimated* the *mean* maximum mass-transfer rate (which goes into the definition of η) since there have been times during which the accretion luminosity was higher. If we have *under-estimated* the rate (we have no means of knowing whether there aren't *always* some spots in the L_1-region), then again the spot filling factor is larger, not smaller.

The resulting simulated appearance of the spotted surface of AM Her near the L_1-point (Fig. 6) shows how extremely spotted the secondary star in AM Her must be – at least at one special location – if the mean density of spots is roughly constant.

5. Discussion

There are four possible explanations for the mass-transfer behaviour of the secondary in AM Her.

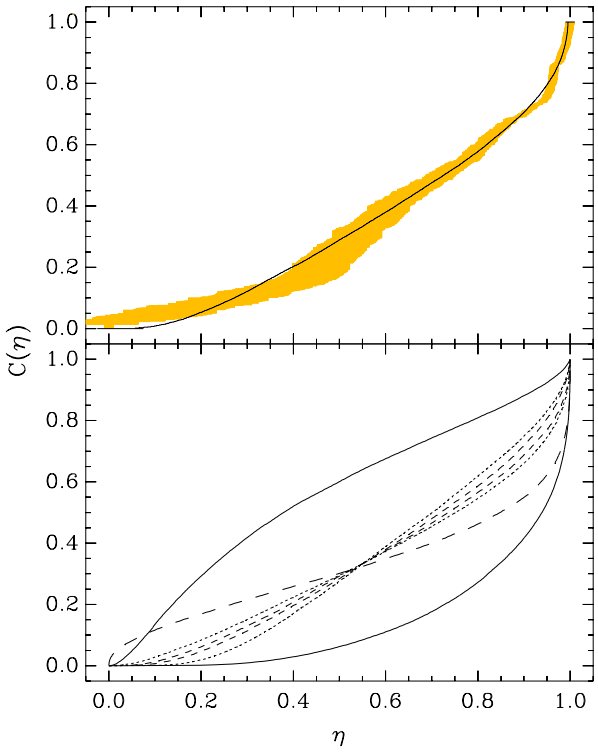

Fig. 5. Top: the observed (filled area) and fitted (solid line) cumulative distribution functions $C(\eta)$ of the spottedness η. Bottom: the effects of individual variations in the parameters on the simulated $C(\eta)$: f=0.33,0.73 (solid line); γ=1.58,2.38 (dotted); $R_{\rm min} = 2.12\,R_{L_1}$ (large dash) and $R_{\rm max} = 2.71, 3.11\,R_{L_1}$ (small dash).

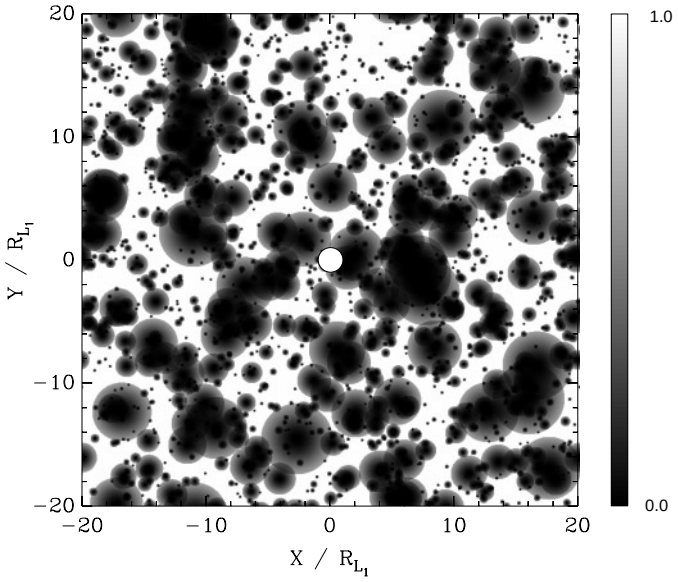

Fig. 6. A simulated spotted surface of the secondary star in AM Her. The circle in the middle represents the size of the mass-transfer nozzle at the L_1-point.

(i) The spottedness of the L_1 region is not untypical.

If the secondaries in CV's have unusually large spot covering fractions over their entire surfaces and very dark spots, one would expect their flux radii to be quite small, i.e. the optically visible surfaces would be smaller than their geometric areas. The low-mass stellar models of Baraffe & Chabrier (1996) show that, for M dwarf masses in the range $0.1 < M/M_\odot < 0.6$, the luminosity goes as $M^{2.3}$. The Roche geometry demands that the mean density of the stars at a given $P_{\rm orb}$ be (roughly) constant, i.e. that $R \propto M^{1/3}$. Thus, the temperature of an M dwarf CV secondary at a given $P_{\rm orb}$ goes as $M^{(2.3-2/3)/4} = M^{0.41}$. The effective temperature of a spotted star with photospheric temperature T and an area filling factor f of its totally dark spots is $(1-f)^{1/4}T$, so the temperature in this case is proportional to $M^{0.41}(1-f)^{-1/4}$. Imagine that we have two systems at the same orbital period and with secondaries with the same spectral class (i.e. T) but one is spotted and the other is not: the spottedness of the spotted star must then be

$$(1-f) \approx \left(\frac{M_{\rm sp}}{M_{\rm un}}\right)^{1.6}, \quad T, P_{\rm orb} = const \tag{9}$$

i.e. the mass and hence the radius of the spotted star must be smaller than the unspotted one with the same spectral type (e.g. for $f = 0.5$, $M_{\rm sp}/M_{\rm un} = 0.6$, $R_{\rm sp}/R_{\rm un} = 0.9$). This effect is increased if the secondaries are transfering material (Kolb & Baraffe 2000) since this causes them to have larger radii at constant mass and hence smaller radii, masses, and later spectral types at constant $P_{\rm orb}$. Deviations of this kind have been seen by Beuermann et al. (1998): CV's above and below the gap tend to be of later spectral type than the equivalent (solar abundance) main-sequence stars of the same mean density. While the systems above the orbital period gap are expected to be out of thermal equilibrium, the stars below the gap should be very near the main-sequence (unless they have evolved to brown dwarfs: Kolb & Baraffe 1999). It is true that the CV secondaries below the gap are individually "indistinguishable from ZAMS stars" (Beuermann et al. 1998), but there is a clear trend: on the average they are over a 1/2 spectral type cooler than expected (about 5–10% in temperature). If this effect is due to massive spottedness, we would predict that the stars are undermassive by the factor

$$\frac{M_{\rm sp}}{M_{\rm un}} \approx \left(\frac{T_{\rm sp}}{T_{\rm un}}(1-f)\right)^{1/1.6} \tag{10}$$

or about 60% for $f = 0.5$.

(ii) The spottedness of the L_1 region is untypical.

If the spottedness of the L_1 region is unusual, there must be some mechanism which preferentially produces magnetic flux around the L_1-point and/or which forces spot groups which appear at higher latitudes to wander down towards the L_1-point. Granzer et al. (2000) have calculated the dynamics of flux tubes within the convective envelope of a rapidly rotating $0.4\,M_\odot$ star and find that spots are most likely to occur at relatively high latitudes. Thus, in order to explain the wide range of mass-transfer rates in AM Her, we need a means of bringing the already emergent flux down to the L_1-point: we will present a description of such a process elsewhere (Hessman & Gänsicke 2000, in preparation).

(iii) The spots are not very dark.

In this case, the secondaries need not be particularly spotted if the magnetic fields are not too strong. However, if the magnetic fields are small, then little depression of the stellar surface occurs and we would not expect to see dramatic changes in the mass-transfer rates. The temperature difference and magnetic field strength can be crudely estimated by shifting the atmospheric structure of an M4 giant ($\log g$ near the L_1-point is considerably reduced from that of a dwarf) down in radius until the density equal to that of the high-state stream ($\sim 2 \cdot 10^{-7}\,\mathrm{g\,cm^{-3}}$) has been reduced by a factor of 20. Using the NextGen models of Hauschildt et al. (1999), we estimate magnetic fields of $\sim 800\,\mathrm{G}$ and corresponding temperature drops by roughly $500\,\mathrm{K}$: these are exactly the fields and dark spots expected from a rapidly rotating and magnetically active M star.

(iv) The secondaries are only moderately spotted.

If the global spottedness is not uniformly high, we need long-term large variations of the magnetic field strengths *at the L_1-point* on the late M dwarfs of polars to produce long-term extended low- and high-states. The fully convective secondaries in most AM Her stars (i.e. below the period gap) are – according to standard dynamo theory – not supposed to show global solar-like magnetic cycles (e.g. Schüssler 1975; Küker & Rüdiger 1999) even though they are expected to be highly magnetic (e.g. like normal M dwarf flare stars). However, the M4 secondary in AM Her (Beuermann et al. 1998) may be just slightly above the mass-limit of $\sim 0.2\,\mathrm{M}_\odot$ where the radiative core of a CV secondary disappears (Kolb & Baraffe 2000): the estimates for the primary mass and binary mass-ratio suggest $M_2 \approx 0.24$–$0.30\,\mathrm{M}_\odot$. Thus, AM Her's secondary may indeed show solar-type activity cycles which could show up as long-term variations in $\dot{\mathrm{M}}$. The period of solar-like cycles in late-type stars can be crudely expressed by the function (Ossendrijver 1997)

$$P_{\mathrm{cycle}} \;\approx\; 11^{\mathrm{yr}} \left(\frac{R_{\mathrm{core}}}{0.7\mathrm{R}_\odot}\right)^2 \left(\frac{\mathcal{D}}{\mathcal{D}_\odot}\right), \quad D \gg 1 \tag{11}$$

where $\mathcal{D}$ is the dynamo number and $\mathcal{D}_\odot \approx 18$. The dynamo number is proportional to the angular velocity difference in the over-shoot region between the radiative core and the convective envelope, the "α"-parameter of the "$\alpha - \Omega$" dynamo, and the cube of the core size, R_{core}. The cycle period and dynamo number of AM Her's small but rapidly rotating M-dwarf secondary would be considerably reduced by the small radius of the hypothetical radiative core ($\sim 0.1 R_*$) but this effect might be more than compensated by the rapid rotation of the envelope ($P_{\mathrm{rot}}(\mathrm{Sun})/P_{\mathrm{orb}}(\mathrm{AM}) \;\approx\; 200$) if the radiative core is sufficiently slowly rotating. Indeed, there is a vague hint of a potential magnetic period in AM Her: the periods of quasi-steady accretion (best seen in Fig. 1) around JD 2444000, 2447000, and 2450000 might suggest a period of ~ 3000 days or $\sim$8 years, corresponding to a dynamo number $\mathcal{D} \approx 100$, i.e. well above that of the sun. Given that the angular velocity difference across the over-shoot region is unlikely to be greater than Ω_{orb}, this implies an anomalously low value of α.

A more likely explanation – certainly for most short period polars whose secondaries are undoubtably fully convective – is that the long-term mass-transfer variations are produced by the slow drift rather than oscillation of a global field produced by an α^2-dynamo (Rädler 1986). The numerical simulations by Küker & Rüdiger (1999) suggest that the very low Rossby-numbers of polar secondaries,

$$Ro \;\equiv\; P_{\mathrm{orb}}/\tau_{\mathrm{conv}} \;\sim\; 10^{-3} \tag{12}$$

(τ_{conv} is the convective turnover time) will produce a magnetic surface configuration resembling that of a dipole tilted into the orbital plane. The long-term high and low states would then be caused by the very slow drift of a quasi-dipolar spot group in and out of the L_1-region. The moment of inertia of the highly magnetic white dwarf is so small, that the rotation of a large-scale field on the secondary can induce a rotation of the white dwarf as well, producing shifts in the phasing of the accretion phenomena. Fortunately, the synchronisation timescales of the few known (highly) asynchronous polars are of the order of hundreds of years (Mouchet et al. 1999) – much longer than the mass-transfer variations seen in AM Her and other polars to date – so the effect is probably negligible. This explanation for the mass-transfer variations predicts that all polars will show quasi-periodic mass-transfer cycles when observed for a long enough time - the observations of AM Her itself suggest decades.

Whatever the mechanism is which changes the amount of magnetic flux present at the L_1-point, this result casts a very different light on the origin of short- and long-term mass-transfer variations in all types of CV's. While global radius variations due to, e.g., irradiation of the secondary (King et al. 1995) can change the maximum possible mass-transfer rates, this very long-term effect (10^3–10^4 years) will not be easily discerned on the short-term if the observed rates are dominated by changes in the number, sizes, form, and filling factors of the spots on much shorter timescales (unless the mechanism simultaneously changes the spottedness).

Since there is no reason to assume that the mass-transfer variations seen in AM Her are *not* present in non-magnetic systems with similar periods, the same mechanism should be affecting the light curves of novalikes and dwarf novae as well: we have applied the mass-transfer history of AM Her to the latter in another paper (Schreiber et al. 2000).

Acknowledgements. We would like to thank D. Schmitt for many enlightening discussions on the physics of dynamos and the anonymous referee for helpful comments. We gratefully acknowledge the dedicated efforts of variable star observers around the world whose observations made this analysis possible.

References

Baraffe I., Chabrier G., 1996, ApJ 461, 51
Beuermann K., Baraffe I., Kolb U., Weichhold M., 1998, A&A 339, 518
de Martino D., Gänsicke B.T., Matt G., et al., 1998, A&A 333, L31
Gänsicke B.T., Beuermann K., de Martino D., 1995, A&A 303, 127

Gänsicke B.T., Hoard D.W., Beuermann K., Sion E.M., Szkody P., 1998, A&A 338, 933
Granzer Th., Schüssler M., Caligari P., Strassmeier K.G., 2000, A&A 355, 1087
Hauschildt P.H., Allard F., Ferguson J., Baron E., Alexander D.R., 1999, ApJ 525, 871
Hessman F.V., 2000, In: Charles P., King A., O'Donoghue D. (eds.) Proc. Brian Warner Symposium, New Astronomy Reviews, Elsevier Science, in press
King A.R., Frank J., Kolb U., Ritter H., 1995, ApJ 444, L37
Kolb U., Baraffe I., 1999, MNRAS 309, 1034
Kolb U., Baraffe I., 2000, In: Charles P., King A., O'Donoghue D. (eds.) Proc. Brian Warner Symposium, New Astronomy Reviews, Elsevier Science, in press
Küker M., Rüdiger G., 1999, A&A 346, 922
Leach R., Hessman F.V., King A.R., Stehle R., Mattei J., 1999, MNRAS 305, L225
Livio M., Pringle J.E., 1994, ApJ 427, 956
Lubow S.H., Shu F.H., 1975, ApJ 198, 383
Meyer F., Meyer-Hofmeister E., 1983, A&A 121, 29
Mouchet M., Bonnet-Bidaud J.-M., de Martino D., 1999, In: Hellier C., Mukai K. (eds.) Annapolis Workshop on Magnetic Cataclysmic Variables. ASP Conf. Ser. 157, p. 215
Ossendrijver M., 1997, A&A 323, 1510
Paerels F., Heise J., van Teeseling A., 1994, ApJ 426, 313
Press W.H., Teukolsky S.A., Vetterling W.T., Flannery B.P., 1992, Numerical Recipes: The Art of Scientific Computing. 2nd Ed., Cambridge Univ. Press
Rädler K.-H., 1986, Astron. Nachr. 307, 89
Schreiber M., Gänsicke B., Hessman F.V., 2000, A&A 358, 221
Schüssler M., 1975, A&A 38, 263
Warner B., 1999, In: Hellier C., Mukai K. (eds.) Annapolis Workshop on Magnetic Cataclysmic Variables. ASP Conf. Ser. 157, p. 63
Zhang E.-H., Robinson E.L., Nather R.E., 1987, ApJ 321, 813